JOURNAL OF VIROLOGY, Nov. 1994, p. 7458–7466
0022-538X/94/$04.00+0

Vol. 68, No. 11

Map Locations of Mouse Hepatitis Virus Temperature-Sensitive Mutants: Confirmation of Variable Rates of Recombination

KAISONG FU[1] AND RALPH S. BARIC[1,2]*

Department of Epidemiology, Program in Infectious Diseases,[1] and Department of Microbiology and Immunology,[2] University of North Carolina, Chapel Hill, North Carolina 27599-7400

Received 23 May 1994/Accepted 16 August 1994

Using standard genetic recombination techniques, studies in our laboratory suggest that recombination rates are very high and vary in different portions of the mouse hepatitis virus (MHV) genome. To determine the actual recombination frequencies in the MHV genome and localize the nucleotide boundaries of individual viral genes, we have sequenced temperature-sensitive and revertant viruses to identify the location of specific mutant alleles. Complementation group F RNA$^+$ *ts* mutants (LA7, NC6, and NC16) each contained a unique mutation which was tightly linked to the *ts* phenotype and resulted in a conservative or nonconservative amino acid change in the MHV S glycoprotein gene. In agreement with previous recombination mapping studies, the mutation in LA7 and NC6 mapped within the S1 domain while NC16 mapped within the S2 domain. To determine the map coordinates of the MHV polymerase genes, several RNA$^-$ mutants and their revertants belonging to complementation groups C (NC3 and LA9) and E (LA18 and NC4) were also sequenced. Mutations were identified in each virus that were tightly linked to the *ts* phenotype and resulted in either a conservative or nonconservative amino acid change. The group C allele spanned the ORF 1a/ORF 1b junction, while the group E mutants mapped at the C terminus of ORF 1b about 20 to 22 kb from the 5′ end of the genome. Mutation rates, calculated from the reversion frequencies of plaque-purified *ts* viruses requiring a single nucleotide alteration for reversion, approached 1.32 (± 0.89) × 10^{-4} substitutions per nucleotide site per round of template copying. Detailed recombination mapping studies across known distances between these different *ts* alleles has confirmed that homologous recombination rates approached 25% and varied within different portions of the MHV genome.

Mouse hepatitis virus (MHV), a member of the family *Coronaviridae*, contains a single-stranded nonsegmented plus-polarity RNA of about 32 kb in length (28, 39). The genomic RNA is surrounded by a helical nucleocapsid structure containing multiple copies of a 50-kDa phosphoprotein (N) (1, 47). The helical nucleocapsid is contained within a lipid envelope containing two virus-specific glycoproteins: the 180-kDa S and the 23-kDa M glycoproteins (50). Some strains of MHV contain a 65-kDa hemagglutinin esterase (HE) (32, 46).

The MHV RNA polymerase genes are probably encoded in two large open reading frames (ORFs), designated ORF 1a and ORF 1b, in the 5′-most 22 kb of the MHV genome. Although the exact location and number of genetic alleles encoded in gene 1 are not known, sequence analysis suggests that ORF 1a contains a membrane anchoring domain, three cysteine-rich domains, two papain-like protease motifs, and a poliovirus 3C-like protease motif, while ORF 1b contains highly conserved polymerase, helicase, and metal binding motifs typical of viral RNA polymerases (8, 9, 28). Six RNA$^-$ complementation groups of MHV have been isolated, and five of these RNA$^-$ complementation groups map within the 22-kb polymerase region of the MHV genome (5, 25, 29, 34, 43).

In addition to the polymerase genes, the genome of MHV contains six to eight large ORFs which are expressed from subgenomic-length mRNAs (26, 42, 45, 47, 48). These mRNAs are arranged in the form of a nested set structure from the 3′ end of the genome and contain a unique leader RNA sequence at the 5′ end which is derived from the 5′ end of the genome (26, 42, 44, 48). Although still under study, considerable data suggest that the MHV subgenomic mRNAs are initially synthesized by a unique discontinuous "leader priming" transcription mechanism from a full-length negative-strand RNA and subsequently amplified by mRNA replication or transcription from subgenomic negative-stranded RNAs containing anti-leaders (2, 7, 41, 44, 45). Each subgenomic mRNA encodes one or more structural or nonstructural proteins, and a single RNA$^+$ complementation group of MHV-A59 has been isolated which maps within the S glycoprotein gene (15, 47).

During mixed infection, MHV undergoes RNA recombination at high frequency, a phenomenon which is probably mediated by the large size of the genome, discontinuous transcription, and the presence of transcriptionally active subgenomic negative strands which contribute to increased recombination rates at the 3′ end of the genome (5, 6, 15, 24, 30). Recombination between the genomes of nonsegmented RNA viruses also provides a convenient method to determine the location and orientation of distinct genetic loci in the viral genome, and genetic maps of polioviruses, aphthoviruses, and coronaviruses have been resolved (5, 14, 15, 27). Since previous studies have suggested that the recombination frequency may vary in different portions of the MHV genome (15), we identified specific mutations which were tightly linked to the temperature-sensitive (*ts*) phenotype in *ts* mutants of MHV-A59 and determined precise recombination frequencies across known distances in the MHV genome.

MATERIALS AND METHODS

Virus and cell culture. Temperature-sensitive mutants representing the complementation group F RNA$^+$ mutants (NC6, LA7, and NC16) as well as the group C (NC3 and LA9) and group E (LA18 and NC4) RNA$^-$ mutants were used during

* Corresponding author. Phone: (919) 966-3895. Fax: (919) 966-2089.

the course of this study (15, 43). Viruses were plaque purified two to three times, and stocks were propagated at 32°C in 150-cm^2 flasks containing DBT cells as previously described (5, 43). To select for revertants of the group C and group E RNA$^-$ mutants, virus stocks were plaque assayed at 39.5°C and individual plaques were isolated and repurified by plaque assay at the restrictive temperature. Individual stocks of revertant virus were grown in 150-cm^2 flasks at 37°C, and the reversion frequencies were determined by plaque assay at 32 and 39.5°C. Since it proved impossible to directly isolate NC4 revertants at 39.5°C, stock virus was passaged for three passages at 37°C and one passage at 39.5°C, prior to the selection of a single plaque at 39.5°C. After plaque purification as described, virus titers were determined at 32 and 39.5°C by plaque assay.

DBT cells were maintained in Dulbecco's modified essential medium containing 6% fetal calf serum, 1% gentamicin/kanamycin (GIBCO), and 5% tryptose phosphate broth. Plaque assays were performed at either the permissive (32°C) or nonpermissive (39.5°C) temperatures in DBT cells in medium containing 0.8% agarose (BRL). Plates were stained with neutral red at 28 to 36 h postinfection and counted.

Recombination analysis. Recombination frequencies were determined as the percentage of ts^+ progeny virus present following a genetic cross between two different *ts* mutants at the permissive temperature and reported as mean ± standard deviation as previously described (5, 14, 15, 27). Following three to seven independent assays, standardized 1% recombination rates (in base pairs) were first adjusted to 1% by dividing the recombination frequency for each independent assay in a particular cross into the number of nucleotides separating the two distinct genetic markers. Average rates were determined, and all values were reported as mean base pairs ± standard deviation. To determine the overall recombination rate in each region of the MHV genome, we averaged the 1% recombination frequency in base pairs from all the available assays in each particular cross with those from all other crosses between *ts* mutants residing within the polymerase gene (NC3, LA9, LA18, and NC4) (n = 28), within the S glycoprotein gene (NC6, LA7, and NC16) (n = 18), or between the 3′ end of the polymerase gene (group E: NC4 and LA18) and the S glycoprotein gene (group F: NC6, LA7, and NC16) (n = 22). Means ± standard deviations were recorded in each region of the genome. Statistically significant differences in recombination frequencies were identified by the Student t test.

Intracellular RNA isolation and cDNA synthesis. Cultures of DBT cells in 60-mm^2 petri dishes were infected at a multiplicity of infection of 5 with different *ts* mutants and their respective revertants for 1 h. After the addition of medium, intracellular RNA was harvested at 10 h postinfection with RNA-STAT-60 (TEL-test "B", INC) as described by the manufacturer. The purified RNA was precipitated under ethanol, washed, resuspended in TE buffer (10 mM Tris-HCl, pH 7.2, 1 mM EDTA), and used directly as a template for cDNA synthesis.

Briefly, cDNA synthesis was accomplished in a 20-μl reaction mixture containing 1 μg of intracellular RNA, 4 μl of 5× first strand reaction buffer (BRL), 2 μl of 0.1 M dithiothreitol (BRL), 1 μl of 10 mM deoxynucleoside triphosphate (Pharmacia), 200 U of Moloney murine leukemia virus reverse transcriptase (BRL), and 1 U of RNase inhibitor (Promega) for 1 h at 37°C. The cDNA products were precipitated in ethanol and resuspended in 50 μl of deionized distilled H_2O.

PCR and subcloning strategies. The MHV S glycoprotein and ORF 1b genetic domains were cloned by PCR. Briefly, three unique sets of overlapping primer pairs were used to clone the MHV S glycoprotein gene (15, 31). Seven additional sets of overlapping primer pairs were synthesized from highly conserved regions within the MHV A59/JHM ORF 1a and ORF 1b domains (9, 29) (Table 1). These primer pairs span the entire ORF 1b domain, as well as the 3′-most 1 kb of the ORF 1a and the 5′ end of the HE gene (32). Following cDNA synthesis and 25 cycles of PCR, the DNA products were separated on agarose gels, purified by Geneclean Kit II (Bio101, Inc.) as described by the manufacturer, and used directly for subcloning or sequencing by asymmetric PCR.

TABLE 1. Oligonucleotide primers designed for PCR of ORF 1a and ORF 1b in MHV

Name	Oligomer (5′–3′)	Location (nt)	Direction[a]
P1a	TAGATGAGGCCAAGGC	12369–12384[b]	+
P1b	AAACGGAAGCACCACC	86–71[c]	−
P2a	TGTGACCATGCTGGCAC	1–17[c]	+
P2b	TATCCACCATGGTGGG	1660–1645[c]	−
P3a	GAGGGGAGCTCCGTTG	1555–1570[c]	+
P3b	GGTCTCATCAGTAAAC	3021–3006[c]	−
P4a	TCAGATCCTGGACAGC	2955–3010[c]	+
P4b	ATACGGCGTTACTCCAACTG	4588–4569[c]	−
P5a	GGCCAGACTACACATGAGAG	4489–4508[c]	+
P5b	CATTACAGCCAGGGAGAT	6088–6071[c]	−
P6a	GGAACTGCAATGTGGAT	5996–6012[c]	+
P6b	GCTAGAGCTTCATTACCGC	7073–7055[c]	−
P7a	GCCTTGAACCGAGCCATTA	6989–7007[c]	+
P7b	TTCACAGCCACGACAAGT	26–9[d]	−

[a] +, sequence corresponding to mRNA strand; −, sequence complementary to mRNA strand.
[b] Sequence described by Lee et al. (28).
[c] Sequence described by Bredenbeek et al. (9).
[d] Sequence described by Luytjes et al. (32).

PCR products were also subcloned into pGEM-T vector system I (Promega) as described by the manufacturer. Following ligation, the recombinant plasmid DNAs were transformed into *Escherichia coli* DH5-competent cells (Stratagene) and screened on LB plates containing 50 μg of ampicillin per ml, 100 mM IPTG (isopropyl-β-D-thiogalactopyranoside), and 100 μl of 2% X-Gal (5-bromo-4-chloro-3-indolyl-β-D-galactopyranoside) (USB). Plasmid DNA was isolated and screened for the presence of insert DNA by restriction mapping or oligonucleotide probing.

For asymmetric PCR, 1/25 of the initial PCR product was mixed with primer pairs added at a ratio of 1:100 (Primer A/Primer B = 1/100). Following the addition of deoxynucleoside triphosphates and *Taq* polymerase and 25 PCR cycles, the DNA product was predominantly single-stranded DNA which was used directly for sequencing without further denaturation (55).

Sequence analysis. DNA sequencing was accomplished by the dideoxyribonucleotide chain termination method. For sequencing of double-stranded plasmid DNA, the DNA was denatured with a 1:1 volume of 5 M NaOH for 5 min at 25°C and then precipitated in 4/5 volume of 5 M NH_4OAc and 10× volume of 100% ethanol for 10 min at −80°C. The samples were precipitated by centrifugation and washed twice with 70% ethanol before sequencing. The Sequenase Version 2.0 DNA Sequencing Kit (USB) and [^{35}S]dATP were used for sequencing as described by the manufacturer. The 1.0- to 1.5-kb PCR products amplified with the oligonucleotide primer pairs described in Table 1 were sequenced by using oligonucleotide primers corresponding to nucleotides (nt) 12369 to 12384 or 12872 to 12887, or complementary to nt 12956 to 12941, in ORF 1a (28) or corresponding to nt 1 to 16, 460 to 475, 1050

TABLE 2. Complementation group C, E, and F *ts* and revertant virus titers

Mutant	Titer at temp (°C)		
	32	39.5	39.5/32
RNA^- mutants			
LA18	6.08×10^7	2.43×10^3	4.05×10^{-5}
LA18 R1	2.25×10^7	9.50×10^6	4.02×10^{-1}
LA18 R2	2.20×10^7	2.25×10^7	1.08×10^0
NC3	2.40×10^8	5.50×10^4	2.30×10^{-4}
NC3 R1	2.00×10^8	2.00×10^8	1.00×10^0
NC3 R2	1.90×10^8	1.80×10^8	9.50×10^{-1}
NC4	1.20×10^7	$<10^1$	$<8.30 \times 10^{-7}$
NC4 R1	7.00×10^6	5.2×10^6	0.70×10^{-1}
LA9	8.60×10^7	7.75×10^3	9.68×10^{-5}
LA9 R1	2.85×10^7	1.00×10^7	3.50×10^{-1}
LA9 R2	3.95×10^7	1.40×10^7	3.50×10^{-1}
RNA^+ mutants			
NC16	8.50×10^7	2.30×10^4	2.70×10^{-4}
NC16 R1	8.12×10^7	9.25×10^7	1.10×10^0
NC16 R2	1.00×10^8	9.00×10^7	0.90×10^{-1}
NC6	2.83×10^7	3.52×10^3	1.2×10^{-4}
NC6 R1	2.30×10^7	2.40×10^7	1.00×10^0
NC6 R2	1.57×10^7	2.12×10^7	1.35×10^0
LA7	2.70×10^7	1.00×10^3	3.70×10^{-5}
LA7 R1	6.98×10^7	8.73×10^7	1.25×10^0
LA7 R2	7.25×10^7	7.15×10^7	9.80×10^{-1}

to 1065, 1555 to 1570, 2076 to 2091, 2453 to 2468, 2955 to 2970, 3502 to 3517, 3981 to 3996, 4489 to 4508, 4987 to 5002, 5470 to 5485, 5996 to 6012, 6482 to 6497, 6989 to 7007, 7497 to 7512, or 8015 to 8030, or complementary to nt 86 to 71, 564 to 549, 1113 to 1098, 1660 to 1645, 2140 to 2125, 2558 to 2573, 3021 to 3006, 3550 to 3535, 4052 to 4037, 4588 to 4573, 5052 to 5037, 5504 to 5489, 6088 to 6071, 6508 to 6493, 7073 to 7058, 7527 to 7512, or 8068 to 8053, in ORF 1b (9). Primers complementary to nt 26 to 9 in ORF 2a were also used to sequence the very 3′ end of the polymerase gene (32). The oligonucleotides designed for sequencing the S glycoprotein gene corresponded to nt 2143 to 2160 in A59 gene 2 (32) and nt 642 to 662, 901 to 916, 1449 to 1465, 2078 to 2094, 2549 to 2564, 3012 to 3027, or 3524 to 3540 in A59 gene S. Complementary primers to nt 439 to 424, 677 to 662, 985 to 970, 1498 to 1481, 2115 to 2103, 2558 to 2537, 3078 to 3063, 3567 to 3551, or 4023 to 4008 were also used in the S gene (31).

RESULTS

Temperature-sensitive and revertant virus of the C, E, and F complementation groups of MHV. All of the *ts* mutants used in this study have been isolated and characterized previously in our laboratory (5, 15, 43). Identification of the mutant allele in MHV *ts* viruses is complicated by the large size of the viral genome (31.6 kb) including a ~22-kb polygenic polymerase region at the 5′ end of the genome which encodes six or more distinct genetic domains functioning in RNA synthesis (5, 25, 29, 34, 39, 43). To simplify this problem, we initially focused our studies on the RNA^+ *ts* mutants which mapped in the S glycoprotein gene of MHV and the RNA^- *ts* mutants which were probably located near the 5′ and 3′ ends of the polymerase gene in ORF 1b by recombination mapping techniques (5). Since infectious vectors for MHV have not been developed, several revertant viruses were isolated by plaque purification at the restrictive temperature for LA9, NC3, and LA18 to assist in the identification of the mutant allele. Revertants of NC4 proved very difficult to isolate and required passage of the virus at 37°C (three times) and 39°C (once) prior to the isolation of a single plaque at 39°C. Revertants of the RNA^+ *ts* mutants LA7, NC6, and NC16 have been previously published (15).

Revertant viruses had similar titers, produced syncytia, and were of the RNA^+ phenotype when assayed at both permissive and restrictive temperatures (Table 2). When cultures were infected and maintained at the restrictive temperature, the replication of *ts* virus was inhibited while the revertant viruses and MHV-A59 wild-type controls grew equally well at both temperatures (15) (data not shown).

Sequence analysis of RNA^+ *ts* and revertant viruses. The strategy for cloning and sequencing the *ts* and revertant viruses is shown in Fig. 1. Unique sets of overlapping primer pairs were developed to clone 1.0- to 1.5-kb stretches of viral RNA in the MHV ORF 1b and S glycoprotein genes by PCR (Table 1). To obviate potential PCR-induced mutations and high polymerase error rates in RNA viruses (19), the PCR product was reamplified by asymmetric PCR and the products were sequenced directly as described in Materials and Methods. This approach ensured that the "master sequence" of the virus population will be determined. After identification of the putative *ts* allele, wild-type A59, *ts* and revertant virus cDNA products were subcloned into plasmid DNA and resequenced to ensure the presence of the mutation or wild-type sequence in independent clones. For the RNA^+ mutants (LA7, NC6, and NC16), the entire S glycoprotein gene was sequenced in *ts* and revertant viruses. For the RNA^- mutants (NC4, LA18, LA9, and NC3), the entire ORF 1b region of the polymerase gene was sequenced in *ts* and revertant viruses. In addition, the 3′-most 1 kb of ORF 1a of NC3 and LA9 was also sequenced in the process of identifying the *ts* lesion. In all cases except NC4, at least two independent revertants were sequenced to demonstrate the location of the *ts* allele.

Among the group F RNA^+ mutants, NC6 contained a nucleotide substitution at the 5′ end of the S glycoprotein gene which was tightly linked to the *ts* phenotype and resulted in an

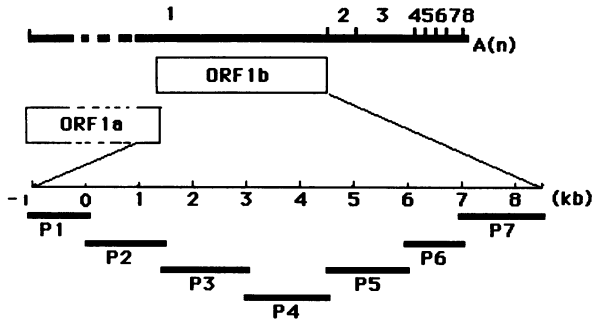

FIG. 1. Cloning and sequencing strategy in the MHV ORF 1a and ORF 1b genes. The organization of the MHV genome is divided into eight large ORFs designated 1 through 8 (8, 26, 28, 42, 47). The MHV polymerase gene is depicted, and the broken line in ORF 1a indicates that the actual size of this genetic domain is much larger than illustrated. PCR-amplified DNAs spanning the C terminus of ORF 1a and the entire ORF 1b region were obtained by using MHV-specific overlapping primer pairs (9), and the PCR products were used as templates for sequencing.

TABLE 3. Nucleotide locations of the MHV A59 *ts* alleles

ts mutant (location in genome)	nt site	nt change[a]		Amino acid change[a]	
		wt	ts/rev	wt	ts/rev
Group F (S gene)					
NC6	620	A	G	Tyr	Cys
NC6R1			A		Tyr
NC6R2			A		Tyr
LA7	1264	G	T	Ala	Ser
LA7R1			G		Ala
LA7R2			G		Ala
NC16	2502	C	G	Asp	Glu
NC16R1			C		Asp
NC16R2			C		Asp
Group C[b]					
ORF 1a					
NC3	171,172	GC	CG	Gly	Ala
NC3R1			GC		Gly
NC3R2			GC		Gly
ORF 1b					
LA9	355	G	A	Asp	Asn
LA9R1			G		Asp
LA9R2			G		Asp
Group E[b] (ORF 1b)					
LA18	7100	G	A	Arg	Lys
LA18R1			G		Arg
LA18R2			G		Arg
NC4	8427	G	C	Ser	Thr
NC4R1			G		Ser
NC4	8429	C	G	Leu	Val
NC4R1			C		Leu

[a] wt, wild type; ts, temperature-sensitive mutant; rev, revertant.
[b] Sequence reported by Bredenbeck et al. (9).

A-to-G transition at nt 620. The mutation had uniformly reversed to A in revertant viruses. The mutation at nt 620 resulted in a nonconservative replacement of Tyr (TAC) to Cys (TGC) at amino acid 207 in the S glycoprotein of NC6 (Table 3 and Fig. 2). LA7 also contained a single nucleotide change at position 1264 in the S1 domain which was tightly linked to the *ts* phenotype, a G-to-T transversion which resulted in a conservative amino acid change from Ala (GCC) to Ser (TCC) at amino acid 422 (Table 3). In LA7 revertants, this nucleotide change also had reversed to the original wild-type sequence. NC16 contained a single nucleotide change involving a C-to-G transversion at nt 2502 in the S2 domain of the S glycoprotein gene which was linked to the *ts* phenotype and resulted in a conservative amino acid change from Asp (GAC) to Glu (GAG). In revertants of NC16, the mutation had reversed to the parental wild-type sequence (Table 3). The location and orientation of these *ts* mutants in the S glycoprotein gene closely approximated their position as predicted from the genetic recombination map reported previously (15). Several additional nucleotide changes were also noted in each mutant and revertant which were not linked to the *ts* phenotype (Table 4).

Sequence analysis of the RNA$^-$ *ts* and revertant viruses. The group E RNA$^-$ mutants had previously mapped near the 3′ end of the polymerase gene by genetic recombination mapping techniques (5). NC4 contained two nucleotide changes near the 3′ end of the polymerase gene at nt 8427 (G to C) and 8429 (C to G) that were tightly linked to the *ts* phenotype. The mutation at 8427 (C to G) resulted in the replacement of a Ser (AGC) with a Thr (ACC), while the mutation at nt 8429 (C to G) resulted in a Leu (CTA) to Val (GTA) change. Collectively, both mutations were conservative and resulted in changes at amino acids 2728 and 2729 in ORF 1b, respectively (Table 3). Since both nucleotides had changed back to the original wild-type sequence in the NC4 revertant and NC4 complements all other *ts* mutants except several group E mutants, these data suggested that NC4 contained a double mutation affecting the group E genetic function. LA18 contained a single nucleotide substitution at nt 7100, which was tightly linked to the *ts* phenotype and located about 1.4 kb from the 3′ end of the polymerase gene. The G-to-A transition led to a conservative change from Arg (AGA) to Lys (AAA) at amino acid 2286 in ORF 1b. In all revertants of LA18, the mutation had reverted to the wild-type sequence (Table 3, Fig. 2).

Among the group C RNA$^-$ mutants which were thought to contain mutations near the ORF 1a/1b boundary by genetic recombination mapping techniques (5), LA9 contained a single nucleotide change at nt 355 in the ORF 1b domain which was tightly linked to the *ts* phenotype. The mutation resided within the ribosomal frameshifting site which regulates expression of the ORF 1b polyprotein (9). The G-to-A transition resulted in a nonconservative alteration from Asp (GAC) to Asn (AAC). In revertant viruses, the altered nucleotide had reversed back to the wild-type sequence (Table 3). NC3 contained two directly adjacent nucleotide alterations at nt 171 and 172 in ORF 1a which were tightly linked to the *ts* phenotype. The mutations were located just 65 nt upstream from the ribosomal frameshifting site between ORF 1a and ORF 1b (9). The alteration (GC to CG) resulted in a nonconservative change from Gly (GGC) to Ala (GCG) at amino acid 4438 in ORF 1a (29). In revertant viruses, both mutations had changed to the wild-type MHV-A59 sequence (Table 3).

In addition to the identification of mutations which were closely linked to the *ts* phenotype, additional nucleotide changes were found in both *ts* and revertant viruses (Table 4). All of these alterations resulted either in silent mutations that did not change the protein sequence or in nucleotide changes that existed in both *ts* and revertant viruses.

Establishing precise recombination rates in the MHV A59 genome. Recombination frequencies between some of the individual *ts* mutants sequenced in this study have been previously reported (5, 15). However, additional recombination mapping experiments were necessary to completely encompass the spectrum of available crosses between these different combinations of mutants. Each mutant was crossed three to seven times with the other mutants used in the study and standardized to the standard cross. Recombination frequencies are expressed as mean ± standard deviation (Table 5).

To standardize recombination rates across known distances between highly defined *ts* alleles, the nucleotide distances between different *ts* alleles (Table 6) were divided by each individual recombination frequency recorded between a particular cross ($n = 3 - 7$). The standardized 1% recombination rate was then calculated in mean base pairs ± standard deviation for each cross (Table 7). The overall 1% recombination rate across different domains in the MHV genome was calculated by averaging each standardized recombination rate recorded from all of the available crosses involving mutants which mapped in either the S glycoprotein gene (LA7, NC6, and NC16), the polymerase gene (LA9, NC3, LA18, and NC4),

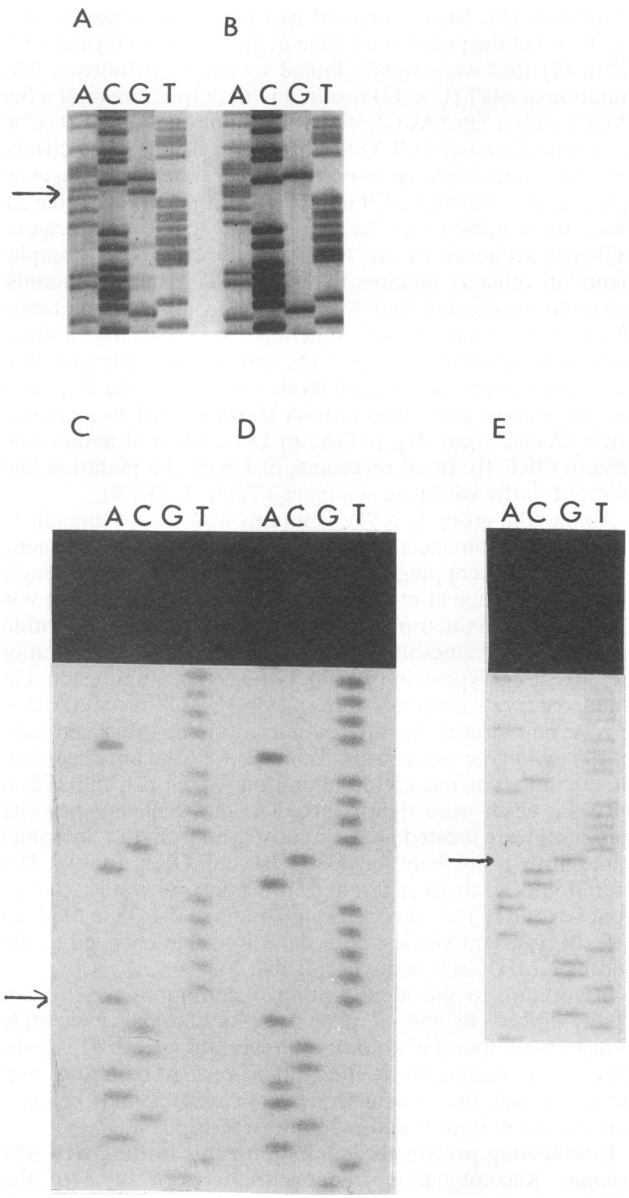

FIG. 2. Identification of mutations linked to the *ts* phenotype. Intracellular RNA was isolated from cells infected with *ts* or revertant viruses, PCR amplified, and sequenced as described in Materials and Methods. The arrows designate the locations of specific mutations linked to the *ts* phenotype. (A) LA18 revertant R1; (B) group E mutant LA18; (C and D) NC6 revertants R1 and R2, respectively; (E) group F mutant NC6. The gels are read from the bottom.

or both domains (NC4, LA18, LA7, NC6, and NC16). Within the S glycoprotein gene the overall average recombination rate was measured as 1%/1,133 ± 762 bp (n = 18) compared with an average mean recombination rate of 1%/5,393 ± 3,558 bp (n = 28) within the polymerase gene. Between the 5′ end of the S glycoprotein gene (group F: NC6, LA7, and NC16) and the 3′ end of the polymerase gene (group E: NC4 and LA18), the average recombination rate was 1%/3,192 ± 1,792 bp (n = 22) (Table 7 and Fig. 3). Statistically significant differences were detected between the rates of recombination measured within the S glycoprotein gene and the polymerase gene ($P <$ 0.0001) and between rates spanning the 5′ end of the S gene and 3′ end of polymerase gene as compared to rates within the polymerase gene ($P < 0.02$) or the S glycoprotein gene ($P <$ 0.0001). To account for the presence of the double *ts* phenotype that would not be detected under our recombination assay conditions (15), the average recombination rate in base pairs would probably be twofold the reported average values (Fig. 3).

TABLE 4. Additional mutations in MHV A59 *ts* and revertant viruses

ts mutant	Location in genome (nt)	nt change[a]			Amino acid change[a]		
		wt	ts	rev	wt	ts	rev
Group F (S gene)							
NC6	131	A	C	C	Glu	Asp	Asp
NC6	514	C	T	C	Gln	Gln	Gln
LA7	2069	G	C	G	Gln	Gln	Gln
NC16	2242	T	C	T	Tyr	Tyr	Tyr
NC16	2275	G	C	G	Gly	Gly	Gly
Group C/E[b] (ORF 1b)							
NC3	209	A	G	G	Glu	Val	Val
LA9	3056	G	A	G	Leu	Leu	Leu
LA18	7112	C	T	T	Ser	Phe	Phe

[a] wt, wild type; ts, temperature-sensitive mutant; rev, revertant.
[b] Sequence as reported by Bredenbeck et al. (9).

DISCUSSION

We have isolated and characterized a panel of *ts* mutants of MHV A59 which were divided into five RNA^- complementation groups and one RNA^+ complementation group and have been mapped by standard genetic recombination techniques (5, 15, 43). These studies have suggested that the RNA^- and the RNA^+ complementation groups of MHV resided within the 22-kb polygenic polymerase region at the 5′ end of the genome and the S glycoprotein gene, respectively, and suggested that the recombination frequency of MHV was among the highest in the nonsegmented RNA viruses (5, 14, 15, 27).

In this study, *ts* and revertant viruses were sequenced to identify specific mutations which correlated with the *ts* phenotype. While this approach suffers from the practical limits of sequencing the entire 32-kb genome in each mutant and the lack of infectious vectors to prove whether a specific mutation encodes the *ts* phenotype, a variety of data suggest that the mutations identified in this study are tightly linked to and probably represent the *ts* allele. Each mutation was present in *ts* but not in revertant viruses. In each case, the location of the *ts* allele corresponded to its putative domain as predicted by standard genetic recombination mapping techniques (5, 15). For example, the predicted orientation and location of the RNA^+ mutants, 5′-NC6-LA7-NC16-3′, was confirmed by sequence analysis with NC6 and LA7 residing in the S1 domain and NC16 in the S2 domain of the S glycoprotein gene. The location of mutants in both the C and E complementation groups were also close to the site predicted from the genetic recombination map (5). Importantly, RNA recombinant viruses, isolated between LA7 and wild-type JHM following selection at 39°C, contained crossover sites which were within 100 bp of (25%) or completely replaced (75%) the LA7 mutation with heterologous JHM sequences (3, 33). While these data provide a strong link between individual mutations

TABLE 5. Recombination frequencies between MHV-A59 *ts* mutants[a]

Mutant	Recombination frequency[b]					
	NC3	LA18	NC4	NC6	LA7	NC16
LA9	0.1 ± 0.09	3.1 ± 1.80	2.2 ± 0.56	5.13 ± 0.97	4.5 ± 0.80	ND
NC3		0.84 ± 0.21	1.67 ± 0.70	5.5 ± 2.10	3.74 ± 2.30	ND
LA18			0.91 ± 0.90	0.9 ± 0.20	1.2 ± 0.30	4.6 ± 0.60
NC4				0.78 ± 0.21	1.40 ± 0.40	1.30 ± 0.10
NC6					0.2 ± 0.02	2.8 ± 0.90
LA7						3.0 ± 1.20

[a] $N = 3$ to 7.
[b] Mean ± standard deviation. ND, not done.

and the *ts* allele, definitive proof must await the development of MHV infectious clones.

The *ts* mutants utilized in this study were isolated in separate experiments using either 5-fluorouracil (LA18 and NC16) or 5-azacytidine (LA7, NC6, NC3, NC4, and LA9) as mutagen and caused point mutations that result in conservative (structurally similar) or nonconservative (structurally dissimilar) amino acid changes in the protein sequence (43). Interestingly, 5-fluorouracil, which should result in changes from T(U) or A to other nucleotides (G or C) in the RNA sequence, was not detected in LA18 and NC16. In contrast, 5-azacytidine, which causes a substitution of C or G with other bases, was evident in *ts* LA7, NC4, LA9, and NC3 but not in NC6. Similar results were reported with Sindbis virus *ts* mutants in which the mutation could not always be equated with the mechanism of action of the selecting mutagen, suggesting that the mutation may have been caused by RNA polymerase error (17, 18).

It is well documented that viral RNA-dependent RNA polymerases do not contain proofreading capabilities and, consequently, have high mutation rates approaching 10^{-3} to 10^{-5} per round of replication (19). Not surprisingly, *ts* mutants of RNA viruses also have reversion frequencies on the order of 10^{-3} to 10^{-5} (25, 29, 34, 43). In the case of polio and Sindbis viruses, reversion to the wild-type phenotype is normally accompanied by reversion at the site of mutation (17, 18, 23). In contrast, *ts* mutants of double-stranded RNA viruses like reoviruses often revert from attenuating second site mutations (40). In this study, all of the MHV *ts* mutants, including those with double mutations, reverted to the wild-type sequence at the site of mutation. Reversion frequencies were usually lower when single rather than double nucleotide changes were required for reversion to the ts^+ phenotype (Table 2). However, NC3 contained a double mutation resulting in a single amino acid change in ORF 1a, yet surprisingly, it had relatively high reversion frequencies on par with other mutants that contained single nucleotide changes. Sequence analysis of the wild-type and NC3 genomes indicates that a single or double nucleotide substitution at either the second and third positions or the third position only in the triplet code could result in a wild-type ts^+ phenotype (MHV-A59-Ala [GCG]; NC3-Gly [GGC]; NC3R1 or NC3R2 revertants-Ala [GCG]; putative ts^+ revertant-Ala [GCC]). It is less clear why the NC3 revertants had completely returned to the wild-type sequence at both positions unless the primary sequence provided some selective advantages following two plaque purifications and the generation of virus stocks. In contrast, NC4 also contained a double mutation in the group E genetic function which altered two amino acids near the C terminus of ORF 1b, and revertants of this virus were virtually impossible to isolate until it had been serially passaged at semipermissive and restrictive temperatures. While we do not have direct evidence, NC4 probably changed to the wild-type phenotype by the accumulation of two independent reversion events which occurred during serial passage.

Although coronavirus polymerase error rates have not been rigorously examined, mutation and reversion frequencies of MHV-A59 and MHV-JHM *ts* mutants generally range from 10^{-3} to 10^{-5}, suggesting that proofreading activities were not present in the MHV polymerase (25, 29, 34, 43). From highly plaque-purified *ts* mutants requiring a single nucleotide alteration at the site of mutation for reversion to the ts^+ phenotype (LA9, NC3, LA18, NC6, NC16, and LA7), we calculated the average polymerase error rate in the MHV genome to approach $1.32 \times 10^{-4} \pm 0.89 \times 10^{-4}$, or about 2.4 mutations per genome round of replication (range, 1.5 to 7.4). This is similar to error rates calculated for other positive-strand RNA viruses (19, 36, 52). It has been suggested that the MHV polymerase may contain a ribonuclease activity which trims leader RNA mismatches at intergenic start sites during "leader-primed" transcription and may also encode an RNA editing function (2, 21). If proofreading or editing activities are encoded in the MHV polymerase, our data suggest that they probably function poorly or not at all in the repair of mismatches incorporated into nascent chains during RNA transcription.

The MHV genomic RNA contains two large ORFs at the 5′ end, and ORF 1b is translated by ribosomal frameshifting as a large ORF 1a/1b polyprotein which is subsequently cleaved by cellular or viral proteases into individual viral proteins (8, 9, 28). It is not clear whether functional viral proteins are encoded which span the ORF 1a/1b junction (28). Previous studies in our laboratory suggest that the group C and E RNA^- mutants encode genetic functions regulating negative- and positive-strand RNA synthesis, respectively (43). The group E genetic function is located between nt 7100 and nt 8427 (amino acids 2274 to 2728 in ORF 1b), while the group C function probably spans the ORF 1a/1b ribosomal frameshifting site since NC3 and LA9 are located at the C and N termini of ORF 1a and ORF 1b, respectively (Fig. 4). These data clearly demonstrate that genetic alleles in ORF 1b function in

TABLE 6. Distances between *ts* alleles

Mutant	Distance (nt)					
	NC3	LA18	NC4	NC6	LA7	NC16
LA9	183	6,845	8,172	10,896	11,540	12,778
NC3		7,028	8,355	11,079	11,723	12,961
LA18			1,327	4,151	4,795	6,033
NC4				2,824	3,468	4,806
NC6					644	1,882
LA7						1,238

TABLE 7. Standardized 1% recombination frequency between different combinations of MHV-A59 *ts* mutants

Mutant	Recombination frequency[a]					
	NC3	LA18	NC4	NC6	LA7	NC16
LA9	6,718 ± 6,093	2,962 ± 1,410	3,930 ± 787	2,145 ± 355	2,683 ± 460	ND
NC3		8,979 ± 1,191	6,006 ± 2,041	2,214 ± 658	4,399 ± 2,238	ND
LA18			4,199 ± 3,274	4,723 ± 450	4,508 ± 1,728	1,054 ± 139
NC4				3,964 ± 1,357	2,723 ± 878	3,721 ± 313
NC6					2,169 ± 1,031	629 ± 331
LA7						615 ± 234

[a] In mean base pairs ± standard deviation. ND, not done.

RNA synthesis. More mutants must be sequenced before reliable estimates of the size and exact location of the functional domains of the group C and E complementation groups can be determined. Since the location of the NC3 and LA9 mutations are not in regions demonstrated to block ribosomal frameshifting in infectious bronchitis virus (11), it is possible that the mutations may ablate proteolytic processing of one or more N-terminal ORF 1b polyproteins (9, 28).

Previous studies in our laboratory have predicted that the overall RNA recombination rates in the polymerase and S glycoprotein genes of MHV approached 1%/1,800–2,500 bp and 1%/575–667 bp, respectively (5, 15). The physical map locations of the seven mutants sequenced in this study allowed us to determine precise recombination rates across defined distances. In the polymerase and S glycoprotein genes, the average recombination rates were about 1%/5,393 ± 3,558 bp and 1%/1,133 ± 762 bp; respectively, which were significantly different ($P < 0.0001$). Recombination rates measured from the S glycoprotein gene to the polymerase gene approached 1%/3,192 ± 1,792 bp, and this was significantly different from rates calculated in either the polymerase ($P < 0.02$) or S ($P < 0.0001$) glycoprotein genes. Assuming that recombination events occur in both directions and result in the double *ts* phenotype, these results closely parallel previous predictions and clearly demonstrate that variable rates of recombination occur within different regions of the MHV genome. Using the markers identified in this study, we can also predict the overall recombination frequency in different portions of the MHV genome. Assuming that recombination events also result in the double *ts* phenotype, recombination frequencies approach 8.2% in the 22-kb polymerase gene, ~1.4% across the p30/HE genes (~2.2 kb), and ~7.1% across the ~4.0-kb S glycoprotein gene (Fig. 3). While markers are not available to measure the recombination frequency at the 3′-most ~4.0 kb of the viral genome, it has previously been demonstrated that recombination events at the 3′ end of the genome can be detected in the absence of selective markers (20). Thus, it seems likely that the recombination frequency will approach or exceed rates in the S glycoprotein gene, approximately 7 to 8% or more.

Several explanations could account for the increase in the rate of recombination within the MHV genome, including high negative interference, preferred "hot spots" of recombination, and the presence of nested set subgenomic negative strands and subgenomic mRNA which increase the amount of available template for switching (15, 24). High negative interference seems unlikely since recombination frequencies did not increase as the physical distance between two *ts* alleles decreased and RNA repair mechanisms have not been demonstrated in MHV (16). Since a progressive, statistically significant increase in the recombination rate was detected from the 5′ to the 3′ end of the genome, these findings are inconsistent with recombination hot spots which predict that similar rates of recombination will be detected 5′ and 3′ to the preferred site. Extensive sequence analysis of RNA recombinant viruses also supports the notion of non-site-specific homologous recombination or the idea that crossover events may occur near UU dimers or in regions of secondary structure in sites chosen to minimize the adverse free energy change involved in template switching (4, 13, 22). It has been reported that a preferred site of recombination exists in MHV between nt 1146 and 1431 in the S glycoprotein gene (3). The locations of the two *ts* mutants LA7 (nt 1264) and LA12 (located ~0.2 recombination units from LA7, or about 250 bp) and the monoclonal antibody neutralization sites (near the C-terminal domain of S1 at nt 1766 or 1950) used to select these recombinants have now been identified (54); the actual distance between the two selective markers was only about 0.5 to 0.8 kb. It seems more likely that the clustering of recombination sites in the S glycoprotein gene was defined by the selective markers used in the study (3).

A more likely explanation for different rates of recombination in the MHV genome is the presence of transcriptionally active subgenomic negative strands and nested set mRNAs which effectively increase the amount of template RNA which can participate in switching by copy choice (15). In support of

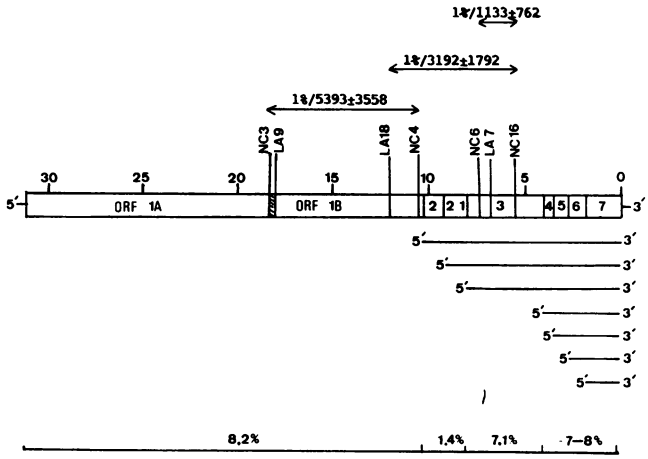

FIG. 3. Recombination rates in different portions of the MHV genome. The relative locations of the MHV-A59 *ts* mutants are superimposed upon the genetic organization and transcriptional strategy of MHV. The group C RNA$^-$ mutants, NC3 and LA9, flank the ribosomal frameshifting site (hatched region) delineating ORF 1a and ORF 1b (9). Standardized 1% recombination rates were determined across the indicated areas as described in Materials and Methods. Overall predicted recombination frequencies for different regions of the MHV genome are shown at the bottom of the figure.

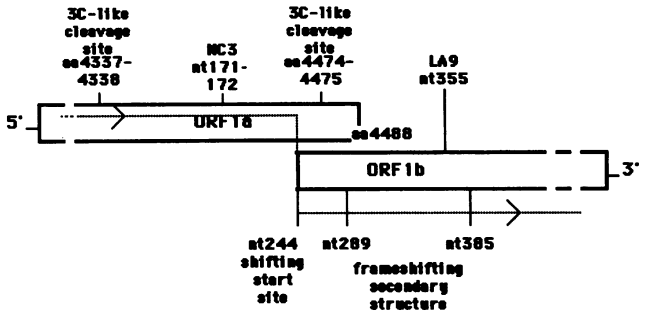

FIG. 4. The location of the group C mutants with respect to the ribosomal frameshifting site. ORF 1a and ORF 1b represent the two large ORFs in the polymerase gene of MHV. The locations of the mutations in LA9 and NC3 are shown relative to the ribosomal frameshifting site (9) and putative poliovirus 3C-like protease cleavage sites (28). These data suggest that complementation group C spans the ORF 1a/1b junction.

this hypothesis, in vitro transcribed mRNAs and 5′-truncated RNA products that were transfected into infected cells participated in recombination (24, 30). In addition, recombinant viruses have also been isolated from persistently infected cells which contain leader RNA sequences inserted into the genomic RNA at highly conserved intergenic sequences suggesting that recombination events occurred between subgenomic-length and full-length mRNA or negative-stranded RNAs (51). Recombination has also been demonstrated between genome-length RNA and subgenomic-length defective interfering RNAs, indicating that differentially sized templates can participate in RNA recombination (53).

The high rate of coronavirus RNA recombination coupled with high polymerase error rates would not only provide a natural mechanism for rapid antigenic variation and evolution within the highly immunogenic structural genes but, as with influenza virus, suggests that these viruses possess significant latent capacity as emerging pathogens (36). Coronaviruses cycle through the human population every couple of years, causing 15 to 20% of the common colds in winter. Occasionally, they are associated with lower respiratory tract infections like bronchitis and pneumonia, and they have been implicated in perimyocarditis and infections of the central nervous system, including multiple sclerosis (37, 49). It is also clear that MHV can rapidly alter its species specificity and infect rats and primates in vivo. The resulting variant viruses produce encephalitis or demyelination in the new host (35, 38). Newly recognized animal coronaviruses include porcine respiratory disease virus and porcine epidemic diarrhea coronavirus (10, 12). Porcine respiratory disease virus probably evolved from porcine transmissible gastroenteritis virus by mutation and recombination, resulting in numerous deletions and mutations in structural and nonstructural genes (12). In contrast, porcine epidemic diarrhea coronavirus is more closely related to the human coronavirus 229E than porcine transmissible gastroenteritis virus, suggesting that it may have evolved from or recombined with human strains (10). The high mutation and RNA recombination rates of coronaviruses suggest that these viruses have the potential to evolve rapidly, transverse the species barrier under the appropriate conditions, and emerge as major pathogens associated with significant morbidity and mortality.

ACKNOWLEDGMENTS

We are grateful to Robert E. Johnston and J. Ed Hall for valuable advice and Wan Chen, Sheila Peel, and Boyd Yount for excellent technical assistance.

This research was supported by grants from the American Heart Association (AHA 90-1112) and the National Institutes of Health (AI-23946) and was performed during the tenure of an Established Investigator Award from the American Heart Association (AHA 89-0193) to R.S.B.

REFERENCES

1. **Armstrong, J., S. Smeekens, and P. Rottier.** 1983. Sequence of the N gene from murine coronavirus MHV-A59. Nucleic Acids Res. **11**:883–891.
2. **Baker, S. C., and M. M. C. Lai.** 1990. An in vitro system for the leader-primed transcription of coronavirus mRNAs. EMBO J. **9**: 4173–4179.
3. **Banner, L. R., J. G. Keck, and M. M. Lai.** 1990. A clustering of RNA recombination sites adjacent to a hypervariable region of the peplomer gene of murine coronavirus. Virology **175**:548–555.
4. **Banner, L. R., and M. M. Lai.** 1991. Random nature of coronavirus RNA recombination in the absence of selection pressure. Virology **185**:441–445.
5. **Baric, R. S., K. S. Fu, M. C. Schaad, and S. A. Stohlman.** 1990. Establishing a genetic recombination map for MHV-A59 complementation groups. Virology **177**:646–656.
6. **Baric, R. S., C. K. Shieh, S. A. Stohlman, and M. M. C. Lai.** 1987. Analysis of intracellular small RNAs of mouse hepatitis virus: evidence for discontinuous transcription. Virology **156**:342–354.
7. **Baric, R. S., S. A. Stohlman, and M. M. C. Lai.** 1983. Characterization of replicative intermediate RNA of mouse hepatitis virus: presence of leader RNA sequences on nascent chains. J. Virol. **48**:633–640.
8. **Bonilla, P. J., A. E. Gorbalenya, and S. R. Weiss.** 1994. Mouse hepatitis virus strain A59 RNA polymerase gene ORF 1a: heterogeneity among MHV strains. Virology **198**:736–740.
9. **Bredenbeek, P. J., C. J. Pachuk, A. F. H. Noten, J. Charite, W. Luytjes, S. R. Weiss, and W. J. M. Spaan.** 1990. The primary structure and expression of the second open reading frame of the polymerase gene of the coronavirus MHV-A59; a highly conserved polymerase is expressed by an efficient ribosomal frameshifting mechanism. Nucleic Acids Res. **18**:1825–1832.
10. **Bridgen, A., M. Duarte, K. Tobber, H. Laude, and M. Ackermann.** 1993. Sequence determination of the nucleocapsid protein gene of the porcine epidemic diarrhoea virus confirms that this virus is a coronavirus related to human coronavirus 229E and porcine transmissible gastroenteritis virus. J. Gen. Virol. **74**:1795–1804.
11. **Brierly, I., P. Digard, and S. C. Inglis.** 1989. Characterization of an efficient coronavirus ribosomal frame-shifting signal: requirement for an RNA pseudoknot. Cell **57**:537–547.
12. **Britton, P., K. L. Mawditt, and K. W. Page.** 1991. The cloning and sequencing of the virion protein genes from a British isolate of porcine respiratory coronavirus: comparison with transmissible gastroenteritis virus genes. Virus Res. **21**:3.
13. **Cascone, P. J., T. F. Haydar, and A. E. Simon.** 1993. Sequences and structures required for recombination between virus-associated RNAs. Science **260**:801–805.
14. **Cooper, P. D.** 1968. A genetic map of poliovirus temperature-sensitive mutants. Virology **35**:584–596.
15. **Fu, K., and R. S. Baric.** 1992. Evidence for variable rates of recombination in the MHV genome. Virology **189**:88–102.
16. **Glickman, B. W., and M. Radman.** 1980. *E. coli* mutator mutants deficient in methylation-instructed DNA mismatch correction. Proc. Natl. Acad. Sci. USA **77**:1063–1067.
17. **Hahn, Y. S., A. Garkovi, C. M. Rice, E. G. Strauss, and J. H. Strauss.** 1989. Mapping of RNA$^-$ temperature-sensitive mutants of Sindbis virus: complementation group F mutants have lesions in nsP4. J. Virol. **63**:1194–1202.
18. **Hahn, Y. S., E. G. Strauss, and J. H. Strauss.** 1989. Mapping of RNA$^-$ temperature-sensitive mutants of Sindbis virus: assignment of complementation groups A, B, and G to nonstructural proteins. J. Virol. **63**:3142–3150.
19. **Holland, J., K. Spindler, F. Horodyski, E. Grabau, S. Nichol, and**

S. Vandepol. 1982. Rapid evolution of RNA genomes. Science **215:**1577–1585.

20. **Keck, J. G., L. H. Soe, S. Makino, S. A. Stohlman, and M. M. C. Lai.** 1988. RNA recombination of murine coronaviruses: recombination between fusion-positive mouse hepatitis virus A59 and fusion-negative mouse hepatitis virus 2. J. Virol. **62:**1989–1998.
21. **Kim, Y.-N., M. M. C. Lai, and S. Makino.** 1993. Site specific sequence repair of coronavirus defective interfering RNA by RNA recombination and edited RNA. Adv. Exp. Med. Biol. **342:**143–148.
22. **King, A. M. Q.** 1988. Preferred sites of recombination in poliovirus RNA: an analysis of 49 intertypic crossover sequences. Nucleic Acids Res. **16:**1705–1723.
23. **King, A. M. Q., S. A. Ortlepp, J. W. Newman, and D. McCahon.** 1987. Genetic recombination in RNA viruses, p. 129–152. *In* R. J. Rowlands, M. A. Mayo, and B. N. Mahy (ed.), The molecular biology of the positive strand RNA viruses. Academic Press, London.
24. **Koetzner, C. A., M. M. Parker, C. S. Ricard, L. S. Sturman, and P. S. Masters.** 1992. Repair and mutagenesis of the genome of a deletion mutant of the coronavirus mouse hepatitis virus by targeted RNA recombination. J. Virol. **66:**1841–1848.
25. **Koolen, M. J. M., A. D. M. E. Osterhaus, G. Van Steenis, M. C. Horzinek, and B. A. M. van der Zeijst.** 1983. Temperature sensitive mutants of mouse hepatitis virus strain A59: isolation, characterization and neuropathogenic properties. Virology **125:**393–402.
26. **Lai, M. M. C., R. S. Baric, P. R. Brayton, and S. A. Stohlman.** 1984. Characterization of leader RNA sequences on the virion and mRNAs of mouse hepatitis virus, a cytoplasmic virus. Proc. Natl. Acad. Sci. USA **81:**3626–3630.
27. **Lake, J. R., R. A. J. Priston, and W. R. Slade.** 1975. A genetic recombination map of foot and mouth disease virus. J. Gen. Virol. **27:**355–367.
28. **Lee, H.-J., C.-K. Shieh, A. E. Gorbalenya, E. V. Koonin, N. La Monica, J. Tuler, A. Bagdzhadzhyan, and M. M. C. Lai.** 1990. The complete sequence (22 kilobases) of murine coronavirus gene 1 encoding the putative proteases and RNA polymerase. Virology **180:**567–582.
29. **Leibowitz, J. L., J. R. de Vries, and M. V. Haspel.** 1982. Genetic analysis of murine hepatitis virus strain JHM. J. Virol. **42:**1080–1087.
30. **Liao, C.-L., and M. M. C. Lai.** 1992. RNA recombination in a coronavirus: recombination between viral genomic RNA and transfected RNA fragments. J. Virol. **66:**6117–6124.
31. **Luytjes, W., P. J. Bredenbeek, J. Charite, B. A. van der Zeijst, M. C. Horzinek, and W. J. Spaan.** 1987. Primary structure of the glycoprotein E2 of coronavirus MHV-A59 and identification of the trypsin cleavage site. Virology **161:**479–487.
32. **Luytjes, W., P. J. Bredenbeek, A. F. H. Noten, M. C. Horzinek, and W. J. M. Spaan.** 1988. Sequence of mouse hepatitis virus A59 mRNA 2: indications for RNA recombination between coronavirus and influenza C virus. Virology **166:**415–422.
33. **Makino, S., J. O. Fleming, J. G. Keck, S. A. Stohlman, and M. M. C. Lai.** 1987. RNA recombination of coronaviruses: localization of neutralizing epitopes and neuropathogenic determinants on the carboxyl terminus of peplomers. Proc. Natl. Acad. Sci. USA **84:**6567–6571.
34. **Martin, J. P., F. Koehren, J. J. Rannou, and A. Kirn.** 1988. Temperature sensitive mutants of mouse hepatitis virus type 3 (MHV-3): isolation, biochemical and genetic characterization. Arch. Virol. **100:**147–160.
35. **Mohanda, D. V., and S. Dales.** 1991. Infection by coronavirus JHM of rat neurons and oligodendrocyte-type 2 astrocyte lineage cells during distinct developmental stages. J. Virol. **65:**5103–5108.
36. **Morse, S. S.** 1994. The viruses of the future? Emerging viruses and evolution, p. 325–335. *In* S. S. Morse (ed.), The evolutionary biology of viruses. Raven Press, Ltd., New York.
37. **Murray, R. S., B. Brown, D. Brian, and G. F. Gabirac.** 1992. Detection of coronavirus RNA and antigen in multiple sclerosis brain. Ann. Neurol. **31:**525–533.
38. **Murray, R. S., et al.** 1992. Coronavirus infects and causes demyelination in the primate central nervous system. Virology **188:**274–284.
39. **Pachuk, C. J., D. J. Bredenbeck, P. W. Zoltick, W. J. M. Spaan, and S. R. Weiss.** 1989. Molecular cloning of the gene encoding the putative polymerase of mouse hepatitis coronavirus strain A59. Virology **171:**141–148.
40. **Ramig, R. F.** 1980. Suppression of temperature-sensitive phenotype in reovirus: an alternative pathway from ts to ts^+ phenotype, p. 633–642. *In* B. N. Fields, R. Jaenisch, and C. F. Fox (ed.), Virology. Animal virus genetics.
41. **Sawicki, S. G., and D. L. Sawicki.** 1990. Coronavirus transcription: subgenomic mouse hepatitis virus replicative intermediates function in RNA synthesis. J. Virol. **64:**1050–1056.
42. **Schaad, M. C., and R. S. Baric.** 1993. Evidence for new transcriptional units encoded at the 3′ end of the mouse hepatitis virus genome. Virology **196:**190–198.
43. **Schaad, M. C., S. A. Stohlman, J. Egbert, K. Lum, K. Fu, T. Wei, Jr., and R. S. Baric.** 1990. Genetics of mouse hepatitis virus transcription: identification of cistrons which may function in positive and negative strand RNA synthesis. Virology **177:**634–645.
44. **Sethna, P. B., M. A. Hofmann, and D. A. Brian.** 1991. Minus-strand copies of replicating coronavirus mRNAs contain antileaders. J. Virol. **65:**320–325.
45. **Sethna, P. B., S.-L. Hung, and D. A. Brian.** 1989. Coronavirus subgenomic minus-strand RNAs and the potential for mRNA replicons. Proc. Natl. Acad. Sci. USA **86:**5626–5630.
46. **Shieh, C.-K., H.-J. Lee, K. Yokomori, N. LaMonica, S. Makino, and M. M. C. Lai.** 1989. Identification of a new transcriptional initiation site and the corresponding functional gene 2b in the murine coronavirus RNA genome. J. Virol. **63:**3729–3736.
47. **Siddell, S.** 1983. Coronavirus JHM: coding assignments of subgenomic mRNAs. J. Gen. Virol. **64:**113–125.
48. **Spaan, W., H. Delius, M. Skinner, J. Armstrong, P. Rottier, S. Smeekens, B. A. M. van der Zeijst, and S. G. Siddell.** 1983. Coronavirus mRNA synthesis involves fusion of non-contiguous sequences. EMBO J. **2:**1839–1844.
49. **Steward, J. N., S. Mounir, and P. J. Talbot.** 1992. Human coronavirus gene expression in the brains of multiple sclerosis patients. Virology **191:**502–505.
50. **Sturman, L., and K. Holmes.** 1985. The novel glycoproteins of coronaviruses. Trends Biochem. Sci. **10:**17–20.
51. **Taguchi, F., T. Ikeda, S. Makino, and H. Yoshikura.** 1994. A murine coronavirus MHV-S isolate from persistently infected cells has a leader and two consensus sequences between the M and N genes. Virology **198:**355–359.
52. **Topal, M. D.** 1988. DNA repair, oncogenes, and carcinogenesis. Carcinogenesis **9:**691–696.
53. **van der Most, R. G., L. Heijnen, W. J. M. Spaan, and R. J. deGroot.** 1992. Homologous RNA recombination allows efficient introduction of site-specific mutations into the genome of coronavirus MHV-A59 via synthetic co-replicating RNAs. Nucleic Acids Res. **20:**3357–3371.
54. **Wang, F. I., J. O. Fleming, and M. M. C. Lai.** 1992. Sequence analysis of the spike protein gene of murine coronavirus variants: study of genetic sites affecting neuropathogenicity. Virology **186:**742–749.
55. **Winship, P. R.** 1989. An improved method for directly sequencing PCR amplified material using dimethyl sulphoxide. Nucleic Acids Res. **17:**1266.